



## Full Length Article

Deactivation mechanism of KCl and K<sub>2</sub>SO<sub>4</sub> poisoned V<sub>2</sub>O<sub>5</sub>/WO<sub>3</sub>-TiO<sub>2</sub> catalyst on gaseous elemental mercury oxidation

Jingyuan Hu, Guangqian Luo\*, Zehua Li, Mengyuan Liu, Renjie Zou, Xian Li, Hong Yao

State Key Laboratory of Coal Combustion, School of Energy and Power Engineering, Huazhong University of Science and Technology, Wuhan, Hubei 430074, China

## ARTICLE INFO

## Keywords:

SCR catalyst  
KCl  
K<sub>2</sub>SO<sub>4</sub>  
Poisoning  
Mercury  
Deactivation

## ABSTRACT

In this paper, the mercury oxidation performance of KCl or K<sub>2</sub>SO<sub>4</sub> poisoned V<sub>2</sub>O<sub>5</sub>/WO<sub>3</sub>-TiO<sub>2</sub> catalysts was investigated. And the poisoned samples were prepared by the incipient-wetness impregnation method. The effects of temperature, catalyst poisoning degree and flue gas composition on the catalyst oxidation were investigated respectively. Results demonstrated that Cl<sup>-</sup> and SO<sub>4</sub><sup>2-</sup> doped catalysts would mitigate the effect of catalyst potassium poisoning on the mercury oxidation. Further research on BET and XRD demonstrated that the catalysts surface did not change significantly after KCl and K<sub>2</sub>SO<sub>4</sub> poisoning. Deactivation on physical side was not the main root cause leading to catalyst deactivation. Hg-TPD (Hg temperature-programmed desorption) results showed that the acidic sites formed by SO<sub>4</sub><sup>2-</sup> could promote the adsorption of Hg<sup>0</sup> on the catalysts surface. XPS results showed that both Cl<sup>-</sup> and SO<sub>4</sub><sup>2-</sup> could promote the formation of surface active O<sub>α</sub>. Based on the experimental results and analysis, the KCl and K<sub>2</sub>SO<sub>4</sub> poisoned V<sub>2</sub>O<sub>5</sub>/WO<sub>3</sub>-TiO<sub>2</sub> catalysts mechanism on mercury oxidation was derived.

## 1. Introduction

Mercury is a topic heavy metal pollutant which, once leaked into the atmosphere, would expand in the human body and destroy the nervous and immune system [1,2]. Due to the high mercury content in coal, coal-fired power plants are considered to be one of the largest sources of mercury emissions [3]. There are three forms of mercury (elemental mercury (Hg<sup>0</sup>), particulate mercury (Hg<sup>p</sup>), divalent mercury (Hg<sup>2+</sup>)) in the coal-fired flue gas [4,5] where Hg<sup>0</sup> is difficult to be removed because it is water insoluble and has high volatility [6,7]. The SCR (Selective Catalytic Reduction) system is the main device for removing nitrogen oxides and oxidizing elemental mercury in the coal-fired power plants. When the flue gas passes through the SCR catalysts, most of the Hg<sup>0</sup> will be oxidized to Hg<sup>2+</sup> and Hg<sup>2+</sup> will be removed by the desulfurization slurry in the WFGD [8,9]. SCR catalysts are the core of the SCR system and the commercial catalysts based on V<sub>2</sub>O<sub>5</sub>/WO<sub>3</sub>-TiO<sub>2</sub> are most widely used in the coal-fired power plants [10–12]. Since the SCR catalysts are operating under high temperature and high dust for a long time, they will gradually be poisoned and then deactivated. As a result, the oxidation efficiency of mercury will also reduce accordingly.

In order to reduce the cost of power generation and the emission control of NO<sub>x</sub> and SO<sub>2</sub> [13,14], many power plants replace a certain proportion of biomass into coal as the fuel source. However, the deactivation rate of SCR catalysts will increase in these power plants.

Previous study showed that [15] its deactivation rate was 2–4 times higher than that of coal-fired power plants, which was mainly caused by potassium in the flue gas. The potassium is mainly present in the form of KCl and K<sub>2</sub>SO<sub>4</sub> in the flue gas emitted from the biomass-burning power plants [16,17]. Zheng et al. [18] investigated the effects of KCl and K<sub>2</sub>SO<sub>4</sub> on commercial vanadium-based catalysts in the laboratory. They found that the potassium salt in the flue gas would block the pores and occupy the Brønsted acid sites on the catalyst surface, thus causing the deactivation of NO reduction. However, few researchers have studied the effect of KCl and K<sub>2</sub>SO<sub>4</sub> poisoning catalysts on mercury oxidation. In fact, due to the existence of KCl and K<sub>2</sub>SO<sub>4</sub> in the catalysts, K<sup>+</sup> will occupy the active sites on the catalysts surface and result in the decrease of the mercury oxidation efficiency, but the different anions Cl<sup>-</sup> and SO<sub>4</sub><sup>2-</sup> may benefit. Zheng [18] and other researchers found that when KCl was deposited on the catalyst surface, K was then combined with the Brønsted acidic sites and Cl<sup>-</sup> was also adsorbed on the catalyst surface [19,20], which might promote the oxidation of Hg<sup>0</sup> by the SCR catalyst. Zhao et al. [21] found that the addition of SO<sub>4</sub><sup>2-</sup> could enhance the strong acidity and redox properties of the catalyst, which might have a certain promoting impact on the mercury oxidation. The study on mercury oxidation by SCR catalysts with KCl and K<sub>2</sub>SO<sub>4</sub> deposited on the surface has important guiding significance for future study of anti-K poisoning catalysts and the arrangement of SCR catalysts in coal-fired power plants.

\* Corresponding author.

E-mail address: [guangqian.luo@mail.hust.edu.cn](mailto:guangqian.luo@mail.hust.edu.cn) (G. Luo).

In this study, the commercial  $V_2O_5/WO_3-TiO_2$  catalysts were impregnated with KCl and  $K_2SO_4$  aqueous solution to emulate the SCR catalyst poisoning process [16,22,23]. We investigated the deactivation performance of mercury oxidation over KCl or  $K_2SO_4$  poisoned samples respectively. The effects of catalyst poisoning on surface morphology were characterized by XRD and BET. Finally, the mechanism on mercury oxidation was detailed after Hg-TPD and XPS tests.

## 2. Materials and methods

### 2.1. Catalysts preparation

The catalysts employed in this study were commercial SCR catalysts  $V_2O_5/WO_3-TiO_2$  (denoted as V/W-Ti) with  $V_2O_5$  (1.9%) and  $WO_3$  (6.5%). The fresh catalysts were ground and sieved to 20–60 mesh before experiments.

The KCl and  $K_2SO_4$  poisoned samples were prepared by the incipient-wetness impregnation method. The detailed steps are as follows: firstly, KCl or  $K_2SO_4$  was mixed into the deionized water to prepare the solution with the  $K^+$  concentration of 1%, 3% and 5% respectively; then the catalysts were immersed in KCl or  $K_2SO_4$  solution and the volume of the impregnation solution was determined based on the water absorption (measured in the lab) of the catalysts; finally, the impregnated catalysts were stirred for 6 h and dried at 110 °C for 12 h, after that, calcined at 350 °C for 3 h in the air.

KCl poisoned catalysts were denoted as KxCV/W-Ti or KxC and  $K_2SO_4$  poisoned catalysts as KxSV/W-Ti or KxS, where x represents the concentration of  $K^+$  in the solution. For example, K1CV/W-Ti represents the sample impregnated with 1% KCl aqueous solution.

### 2.2. Catalyst characterization

The  $K_2O$  content within the samples surface was benchmarked by XRF-1800 of Japanese Shimadzu. And the X-ray tube uses Rh target at rated power of 4 Kw, the test element range is B-H. All the prepared samples were characterized by XRF, and the  $K_2O$  content of the samples on the surface was listed in Table 1. When Samples were treated by KCl and  $K_2SO_4$  solutions with the same  $K^+$  concentration, the  $K_2O$  content on the catalysts surface were also basically the same. That illustrated they had the same potassium poisoning degree. The powder X-ray diffraction (XRD) patterns of the samples were measured by Empyrean of PANalytical B.V., operating at rated power of 9 Kw with Cu-K $\alpha$  radiation. The BET surface area, pore size and pore volume were measured by  $N_2$  adsorption at 77 K using ASAP 2020 of MICROMERITICS. Elemental valence of the sample surface was measured by XPS and the binding energy was referenced according to the C 1s standard peak at 284.8 eV.

### 2.3. Catalyst performance test

The experiment system of  $Hg^0$  removal is shown in Fig. 1. The experiment system includes 4 parts: (1) the simulated flue gas unit; (2) the  $Hg^0$  vapor generator unit; (3) the fixed bed reactor; (4) the  $Hg^0$  monitor unit. The simulated flue gas unit was composed of  $O_2$ ,  $N_2$ , NO,  $NH_3$ , HCl,  $SO_2$  and corresponding mass flow meters. The  $Hg^0$  vapor generator unit mainly controlled the concentration of  $Hg^0$  by the temperature of water bath and the  $Hg^0$  vapor was carried by  $N_2$  to the reactor. The fixed bed reactor comprised a vertical tube furnace and a quartz reactor, and the SCR catalyst powder was fixed in the quartz reactor. The

**Table 1**

The content of  $K_2O$  on catalyst surface (wt%).

Samples	V/W-Ti	K1C	K3C	K5C	K1S	K3S	K5S
Content	0	0.739	1.746	2.313	0.747	1.737	2.489

$Hg^0$  monitor unit consisted of an online mercury analyzer (VM3000, Germany) and a connected computer that continuously monitored the  $Hg^0$  concentration at the outlet.

In this paper, the total flow rate was 1 L/min and the  $Hg^0$  vapor concentration is about  $90 < \mu > g/m^3$ . The oxidation temperature is 200–500 °C. 0.35 g sample was fixed in the reactor during each test and the space velocity is  $75377 h^{-1}$ . The removal efficiency of  $Hg^0$  is calculated by the formula (1):

$$\eta_{\text{removal}} = (Hg_{\text{in}}^0 - Hg_{\text{out}}^0) / Hg_{\text{in}}^0 \times 100\% \quad (1)$$

where  $\eta_{\text{removal}}$  is the  $Hg^0$  removal efficiency,  $Hg_{\text{in}}^0$  is the  $Hg^0$  concentration in the inlet and  $Hg_{\text{out}}^0$  is the  $Hg^0$  concentration in the outlet.

The test of Hg-TPD (Hg temperature-programmed desorption) is as below: (1) 0.35 g sample was placed in the reactor for adsorption at the atmosphere of 6%  $O_2$  (carrier gas:  $N_2$ ) and the temperature of 350 °C. The total flow rate was 1 L/min and the  $Hg^0$  vapor concentration was  $90 < \mu > g/m^3$ ; (2) sweep of the sample with pure  $N_2$  (1 L/min) for 30 min; (3) TPD measurement was conducted from 50 °C to 700 °C at a rate of 10 °C/min.  $Hg^0$  is detected by VM 3000.

## 3. Results and discussion

### 3.1. The NO conversion performance of SCR

The SCR performance was investigated through NO conversion experiment. Fig. 2 shows the NO conversion over V/W-Ti, K1SV/W-Ti, K3SV/W-Ti, K5SV/W-Ti, K1CV/W-Ti, K3CV/W-Ti and K5CV/W-Ti catalysts at different temperatures ranging from 200 °C to 500 °C. The fresh V/W-Ti catalyst showed the highest NO conversion rate peaking at 82.46%. With the increase of the content of KCl or  $K_2SO_4$  doping on the catalysts surface, it was obvious that the NO conversion dropped. NO conversion of K5SV/W-Ti and K5CV/W-Ti was even less than 10% at all temperatures. However, the NO conversion of KCl poisoned catalyst was significantly lower than that of  $K_2SO_4$  poisoned catalyst for the same K content on the surface, because  $SO_4^{2-}$  doped on the catalyst surface would improve the redox performance of the catalyst [21].

When KCl or  $K_2SO_4$  was doped on the catalyst surface, a portion of active sites would be occupied, resulting in a severe poisoning of the catalyst. Different potassium salts on the catalyst surface would result in different deactivation of the V/W-Ti catalysts.

### 3.2. $Hg^0$ removal performance

#### 3.2.1. The effect of temperature

Fig. 3 shows the  $Hg^0$  removal efficiency of V/W-Ti, K1SV/W-Ti and K1CV/W-Ti at 200 °C, 300 °C, 350 °C, 400 °C and 500 °C respectively with a duration time of 12 h. As expected, when the reaction temperature raised from 200 °C to 500 °C, the mercury oxidation efficiency of V/W-Ti and K1CV/W-Ti increased before reduced afterwards. Importantly, when the temperature was between 350 and 500 °C, the mercury oxidation efficiency of all catalysts was above 80%. K1CV/W-Ti with the low degree of KCl poisoning showed the mercury oxidation efficiency slightly lower than that of V/W-Ti. In respect of the K1SV/W-Ti, the mercury oxidation efficiency was 83.46% at the temperature of 200 °C, which was significantly higher than the efficiency of V/W-Ti. This was due to the acid sites formed by  $SO_4^{2-}$  promoting the adsorption of  $Hg^0$  at low temperature. The efficiency rose to 89.37%, 91.95%, 91.2% as the temperature increased to 350 °C, 400 °C, 500 °C respectively, which was also higher than the efficiency of V/W-Ti. This was because that the  $SO_4^{2-}$  manifested the strong redox performance at the high temperature which could facilitate the oxidation of mercury.

#### 3.2.2. The effect of K poisoning degree

Fig. 4 shows the mercury removal efficiency of fresh catalysts (V/W-Ti) and poisoned catalysts (KxSV/W-Ti, KxCV/W-Ti) at 350 °C. As for

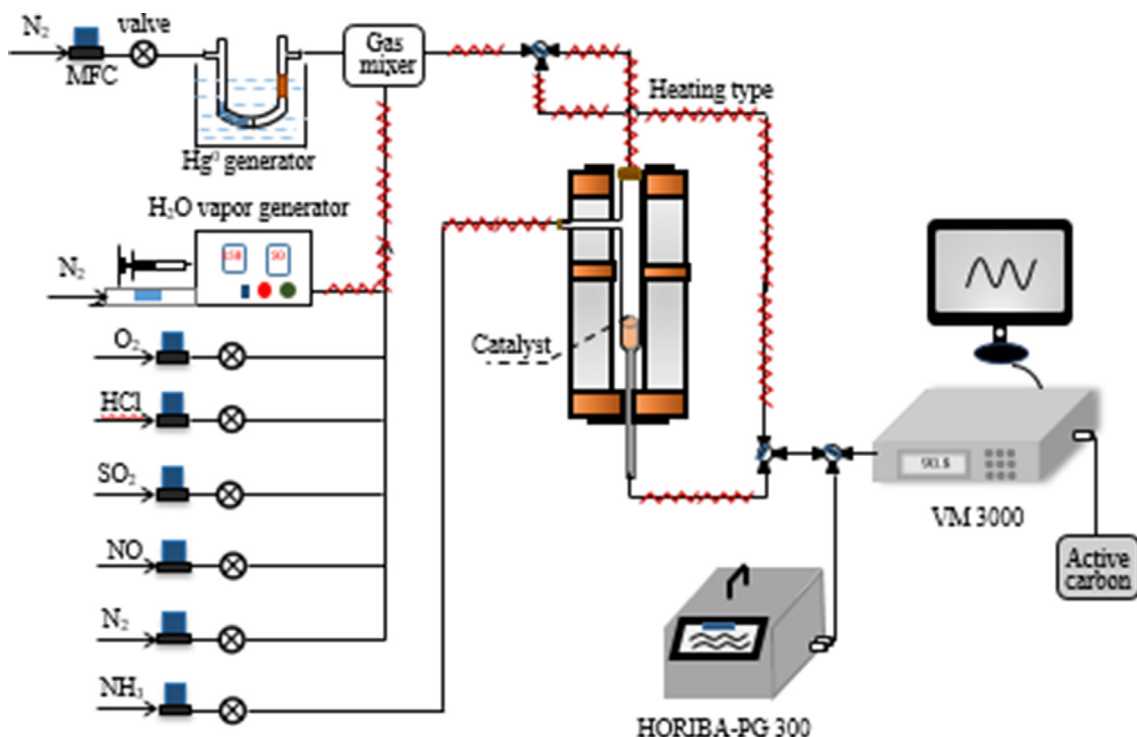


Fig. 1. Experiment system of Hg<sup>0</sup> removal.

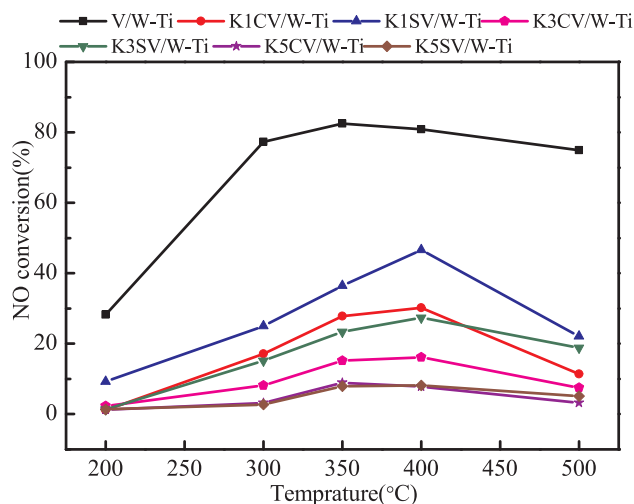


Fig. 2. NO conversion over different catalysts and various temperature (reaction conditions: N<sub>2</sub> as balance gas, 6% O<sub>2</sub>, 400 ppm NO, 400 ppm NH<sub>3</sub>, GHSV = 52736 h<sup>-1</sup>).

KxCV/W-Ti, it was clear that the mercury oxidation efficiency decreased with the KCl poisoning degree increased, because K<sup>+</sup> occupied the acid sites on the catalyst surface. In respect of KxSV/W-Ti, both K1SV/W-Ti and K3SV/W-Ti maintained a high oxidation efficiency with K3SV/W-Ti achieving 94%. It suggested that a slight K<sub>2</sub>SO<sub>4</sub> poisoning could favor the oxidation of mercury due to the SO<sub>4</sub><sup>2-</sup> doped on the catalyst manifesting strong redox performance at high temperatures. However, as the degree of K<sub>2</sub>SO<sub>4</sub> poisoning increased further, the mercury oxidation efficiency of K5SV/W-Ti ended up dropping to 17%. In this case, most acid sites on the catalyst surface were occupied, which greatly mitigated the adsorption of HCl and Hg<sup>0</sup> on the surface.

### 3.2.3. The effect of reaction time

Fig. 5 shows the mercury removal efficiency at the first 50 min of

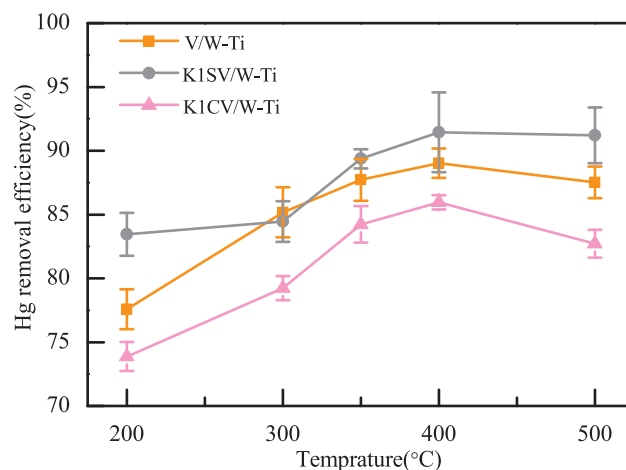


Fig. 3. Hg<sup>0</sup> oxidation over V/W-Ti, K1SV/W-Ti, K1CV/W-Ti catalysts at different temperature (reaction conditions: N<sub>2</sub> as balance gas, 6% O<sub>2</sub>, 12 ppm HCl, GHSV = 75377 h<sup>-1</sup>).

K1,3SV/W-Ti and K1,3CV/W-Ti at 350 °C. The results showed that the oxidation efficiency of K1CV/W-Ti, K1SV/W-Ti and K3SV/W-Ti increased gradually with time until they reached steady state. Among them, K1CV/W-Ti delivered higher oxidation efficiency in the initial transient. This was because that when KCl was loaded on the surface of K1CV/W-Ti, the generated HCl was adsorbed on the catalyst surface [19], so that the HCl concentration on the surface was higher than that on K1SV/W-Ti and K3SV/W-Ti. K3CV/W-Ti achieved the highest efficiency within the initial period with much HCl loaded on the surface, which the oxidation efficiency gradually decreased with time until it was stable because of the HCl consumption within the surface. K3SV/W-Ti had the highest increasing rate, which indicated that SO<sub>4</sub><sup>2-</sup> on the surface of K3SV/W-Ti manifesting strong acidity. Previous study [24] found that Hg<sup>0</sup> could be adsorbed on different acid sites on the catalyst surface, so SO<sub>4</sub><sup>2-</sup> could promote the adsorption of Hg<sup>0</sup> on the catalyst surface.

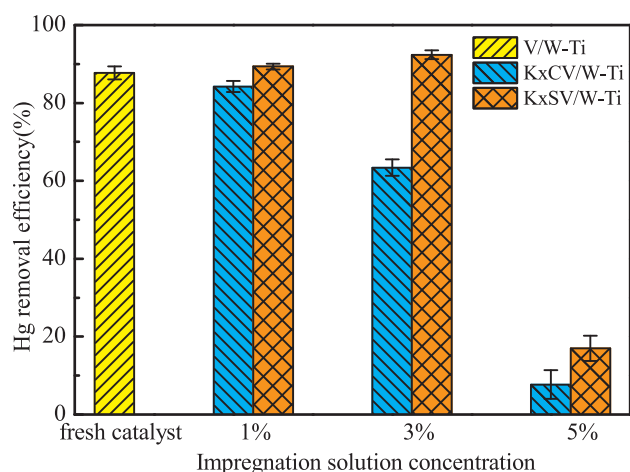


Fig. 4. Hg<sup>0</sup> oxidation over V/W-Ti, KxSV/W-Ti, KxCV/W-Ti catalysts at 350 °C (reaction conditions: N<sub>2</sub> as balance gas, 6% O<sub>2</sub>, 12 ppm HCl, GHSV = 75377 h<sup>-1</sup>).

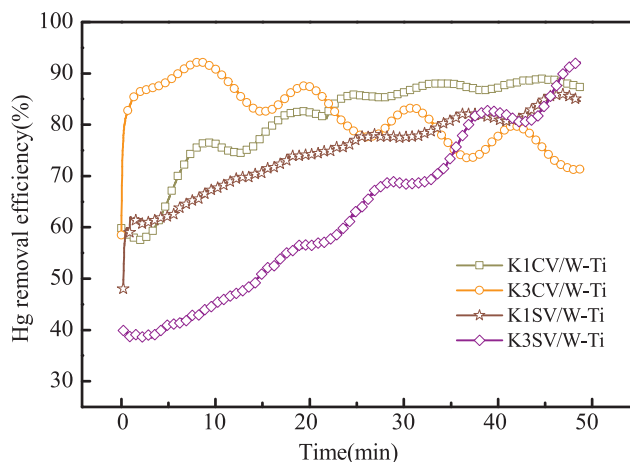


Fig. 5. Hg<sup>0</sup> oxidation over K1,3SV/W-Ti, K1,3CV/W-Ti catalysts at the beginning 50 min (reaction conditions: N<sub>2</sub> as balance gas, 6% O<sub>2</sub>, 12 ppm HCl, GHSV = 75377 h<sup>-1</sup>).

### 3.2.4. The effect of HCl, NO, NH<sub>3</sub>, SO<sub>2</sub> and H<sub>2</sub>O on Hg<sup>0</sup> oxidation

Fig. 6 shows the effect of HCl, NO, NH<sub>3</sub>, SO<sub>2</sub> and H<sub>2</sub>O on Hg<sup>0</sup> oxidation over catalysts. When only 6% O<sub>2</sub> was introduced to the flue gas, the mercury oxidation efficiency of V/W-Ti was 45.93%. This process mainly followed Mars-Maessen mechanism and O<sub>2</sub> could facilitate the lattice oxygen on the catalyst surface [25]. For K1CV/W-Ti, the efficiency was only 35.1% due to the K occupying the acidic sites on the catalyst surface which led to the Mars-Maessen process being significantly inhibited. For K1SV/W-Ti, the efficiency was 44.83% which was higher than K1CV/W-Ti. In this case, SO<sub>4</sub><sup>2-</sup> on the catalyst surface would promote the adsorption of Hg<sup>0</sup>. In the meanwhile, HgSO<sub>4</sub> might also be formed on the surface.

When NO and O<sub>2</sub> were introduced in the flue gas, the mercury oxidation efficiency of catalysts was promoted to some extent. Previous study [26] showed that NO in flue gas would be accumulated within SCR catalyst surface and form a nitrogen-containing complex which promoted the oxidation of Hg<sup>0</sup>. The main reaction process is described as below:

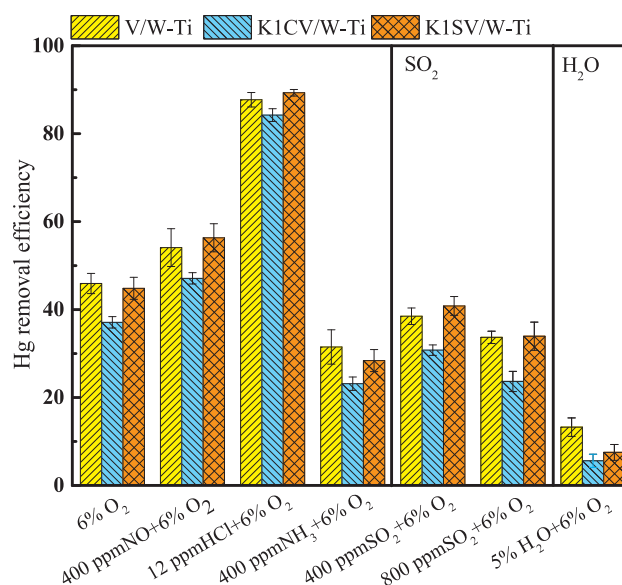
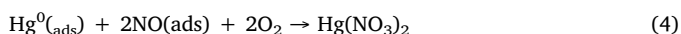
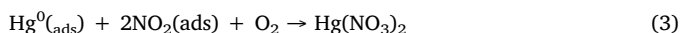
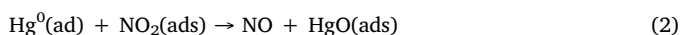


Fig. 6. Effect of HCl, NO, NH<sub>3</sub>, SO<sub>2</sub> and H<sub>2</sub>O on Hg<sup>0</sup> oxidation over V/W-Ti, K1SV/W-Ti and K1CV/W-Ti catalysts (reaction conditions: N<sub>2</sub> as balance gas, GHSV = 75377 h<sup>-1</sup>).

When HCl and O<sub>2</sub> were introduced in the flue gas, the oxidation efficiency of V/W-Ti, K1CV/W-Ti and K1SV/W-Ti were all above 84%. The catalysts mainly followed the Langmuir-Hinshelwood mechanism, where HCl would interact with the lattice oxygen on the surface forming a Cl active site [27]. Then Hg<sup>0</sup> adsorbed on the catalyst surface would be oxidized by the Cl active site to HgCl<sub>2</sub>. The generated HgCl<sub>2</sub> would be released to the flue gas afterwards.

When NH<sub>3</sub> and O<sub>2</sub> were introduced in the flue gas, the oxidation efficiencies of three catalysts were significantly reduced, because that NH<sub>3</sub> would occupy the acidic sites on the catalyst surface [28,29], thereby inhibiting the oxidation process of mercury by the catalyst. Besides, the strong acidic sites formed by SO<sub>4</sub><sup>2-</sup> on the surface of K1SV/W-Ti would also be occupied.

When SO<sub>2</sub> and O<sub>2</sub> were introduced in the flue gas, SO<sub>2</sub> significantly inhibited the mercury oxidation. When 400 ppm SO<sub>2</sub> was added, the efficiencies decreased by 7.5%, 6.8% and 4.0% respectively. While the SO<sub>2</sub> was increased to 800 ppm, the efficiency decreased by 12.3%, 13.5% and 10.9% respectively. Previous research pointed out that [28] SO<sub>2</sub> would be oxidized on the catalyst surface, which would compete with the oxidation of Hg<sup>0</sup>, thereby reducing the oxidation efficiency of elemental mercury.

H<sub>2</sub>O plays an important role in oxy-system coal combustion as reported in our previous study [30,31] and it also has an influence on mercury oxidation. When H<sub>2</sub>O and O<sub>2</sub> were introduced in the flue gas, the inhibition of mercury oxide over the catalysts was more noticeable than that of SO<sub>2</sub> and O<sub>2</sub>. The main reason may be that H<sub>2</sub>O would compete with mercury for the same active sites on the catalyst surface [32].

### 3.3. Characterization of catalysts

#### 3.3.1. BET results

Table 2 shows the pore size distribution of the different catalysts. It can be concluded that when different potassium salts (KCl and K<sub>2</sub>SO<sub>4</sub>) were supported on the V<sub>2</sub>O<sub>5</sub>/WO<sub>3</sub>-TiO<sub>2</sub> catalyst, the BET surface area, pore volume and average pore diameter were slightly reduced compared with the fresh catalyst. At the same time, with the KCl and K<sub>2</sub>SO<sub>4</sub> loaded on the catalyst surface increased, the BET surface area and pore volume decreased slightly, and the average pore size did not show a consistent change. It indicates that when the catalyst was poisoned by

**Table 2**  
Physical properties of the catalysts.

Samples	S <sub>BET</sub> (m <sup>2</sup> /g)	Total pore volume (cm <sup>3</sup> /g)	Average pore diameter (nm)
V/W-Ti	89.52	0.348	16.36
K1CV/W-Ti	88.43	0.343	15.61
K3CV/W-Ti	85.21	0.326	15.32
K5CV/W-Ti	82.67	0.317	15.33
K1SV/W-Ti	88.97	0.334	15.02
K3SV/W-Ti	86.78	0.328	15.12
K5SV/W-Ti	84.87	0.317	14.91

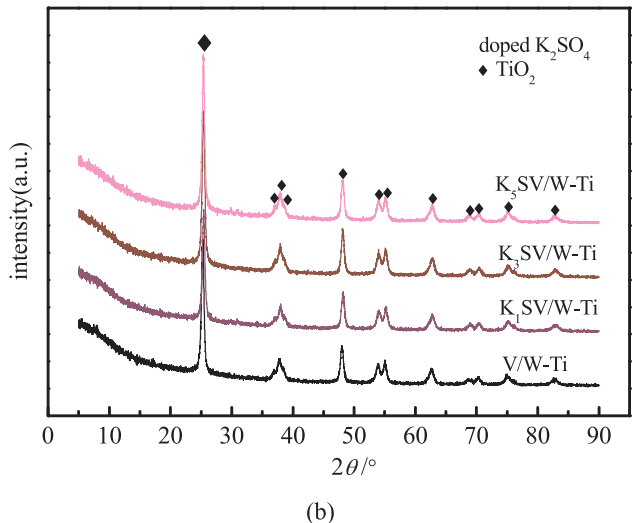
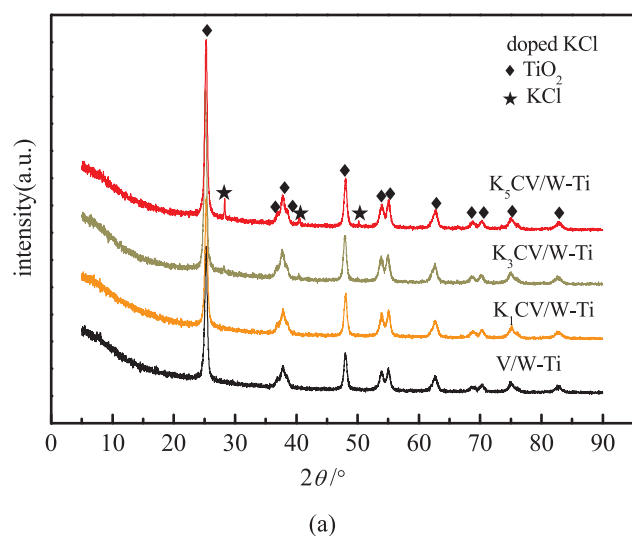


**Fig. 7.** XRD patterns of different catalysts: (a) V/W-Ti, KxCV/W-Ti; (b) V/W-Ti, KxSV/W-Ti.

potassium, it would not have a significant effect on its physical pore structure. The main reason of the change in mercury oxidation efficiency is the different ions deposited on the catalyst surface.

### 3.3.2. XRD results

Fig. 7 shows the XRD patterns of KxCV/W-Ti, KxSV/W-Ti and V/W-Ti. Overall the characteristic peaks of the catalysts (except for K5CV/W-Ti) were nearly the same. The main crystal phase was anatase TiO<sub>2</sub>, and no distinguishable KCl, K<sub>2</sub>SO<sub>4</sub>, WO<sub>3</sub> and V<sub>2</sub>O<sub>5</sub> characteristic peaks were identified, which indicates that they were dispersed in the amorphous form or the small particle crystal phase on the surface of TiO<sub>2</sub>. For

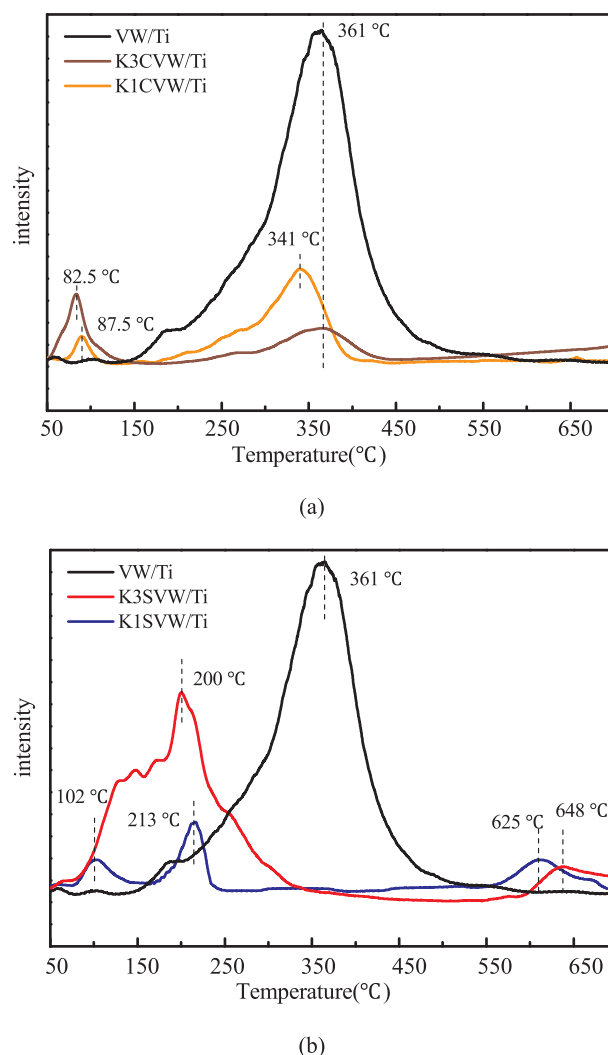


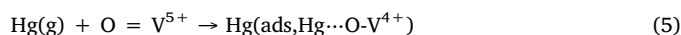
**Fig. 8.** Hg-TPD profiles of catalysts: (a) V/W-Ti, K1,3CV/W-Ti; (b) V/W-Ti, K1,3SV/W-Ti.

K5CV/W-Ti, a small characteristic peak of KCl was found in the figure along with that of TiO<sub>2</sub>, which might be caused by the excessive KCl content. In conclusion, there was no effect on the diffusion of V<sub>2</sub>O<sub>5</sub> on the catalyst surface when the catalyst was poisoned by KCl or K<sub>2</sub>SO<sub>4</sub>.

### 3.3.3. Hg-TPD results

According to the recent research [33], the adsorption of Hg<sup>0</sup> on the catalyst surface was one of the most important steps for the oxidation of mercury by SCR catalyst. Therefore, a Hg-TPD test was conducted to investigate the effect of catalyst poisoning on the adsorption of Hg<sup>0</sup> within the catalyst surface. Fig. 8 shows the Hg-TPD profiles of V/W-Ti, K1CV/W-Ti, K3CV/W-Ti, K1SV/W-Ti and K3SV/W-Ti.

As shown in Fig. 8(a), for the V/W-Ti catalyst, mercury was continuously released from its surface when temperature was higher than 150 °C. A desorption peak was observed at 361 °C. Previous study [29] had confirmed that Hg<sup>0</sup> was adsorbed on the vanadium-titanium catalyst surface in the form of Hg<sup>0</sup>-O-V<sup>4+</sup>, and the process is described below:



Mercury adsorbed on the V/W-Ti catalyst surface may also existed in Hg<sup>0</sup>-O-V<sup>4+</sup> form. For K1CV/W-Ti and K3CV/W-Ti catalysts, the mercury desorption peaked at 87.5 °C and 82.5 °C were caused by the decomposition of weakly adsorbed species [34]; and the mercury

desorption peaks also happened at 341 °C and 361 °C separately, which corresponded to  $\text{Hg}\cdots\text{O}\text{-V}^{4+}$ . As the KCl loaded on the catalyst surface increased, the desorption peak area at high temperature decreased, indicating that the amount of  $\text{Hg}^0$  adsorbed on the surface would decrease with  $\text{K}^+$  occupying the active site during the process of KCl poisoning.

As shown in Fig. 8(b), the desorption peaks of K1SV/W-Ti and K3SV/W-Ti were different from V/W-Ti, which were identified at 213 °C and 200 °C respectively. Previous study [24] reported that  $\text{Hg}^0$  would adsorb on different acid sites on the catalyst surface, which provided a plausible explanation for the desorption peaks that was attributed to the mercury on the strong acid sites formed by  $\text{SO}_4^{2-}$ . The peak area of K3SV/W-Ti was higher than that of K1SV/W-Ti, because the amount of  $\text{SO}_4^{2-}$  loaded on the surface of K3SV/W-Ti was higher and hence more acidic sites being formed. At the same time, there was no peak around 361 °C of K1SV/W-Ti and K3SV/W-Ti, indicating that  $\text{Hg}^0$  in the flue gas inclined to combine with the  $\text{SO}_4^{2-}$  formed acid sites on the catalyst surface. It was also found that K1SV/W-Ti and K3SV/W-Ti peaked at 625 °C and 648 °C respectively which was attributed to  $\text{HgSO}_4$  [35], and it could promote the oxidation of  $\text{Hg}^0$  on the surface of K1SV/W-Ti and K3SV/W-Ti.

### 3.3.4. XPS of $\text{O}_{1s}$

To further reveal the mechanism, the XPS tests were carried out in different catalysts, and the results are shown in Fig. 9. The peaks of each catalyst in the range of 529.3–530.0 eV corresponded to the lattice oxygen  $\text{O}_\beta$  on the surface of the catalyst. The peaks in the range of 531.3–532.9 eV corresponded to the weakly bound oxygen and chemisorbed oxygen  $\text{O}_\alpha$  on the catalyst surface [36]. The  $\text{O}_\alpha$  could greatly promote the oxidation of  $\text{Hg}^0$ . Therefore, the higher the ratio of  $\text{O}_\alpha/(\text{O}_\alpha + \text{O}_\beta)$  in the catalyst, the stronger the ability of the catalyst to oxidize mercury [37]. As shown in Fig. 9, when KCl was loaded on the catalyst surface, the  $\text{O}_\alpha$  ratio decreased from 32.00% (V/W-Ti) to 20.85% (K1CV/W-Ti) and 25.47% (K3CV/W-Ti), due to K occupying the active sites, which was consistent with previous study [23]. However, the ratio of  $\text{O}_\alpha$  in K3CV/W-Ti was obviously higher than that of K1CV/W-Ti, which indicated that there were new chemisorbed oxygen species formed on the surface. They were mainly caused by the HCl that was generated by the process of KCl poisoning. The reactions between HCl and vanadium oxides are as follows [38]:

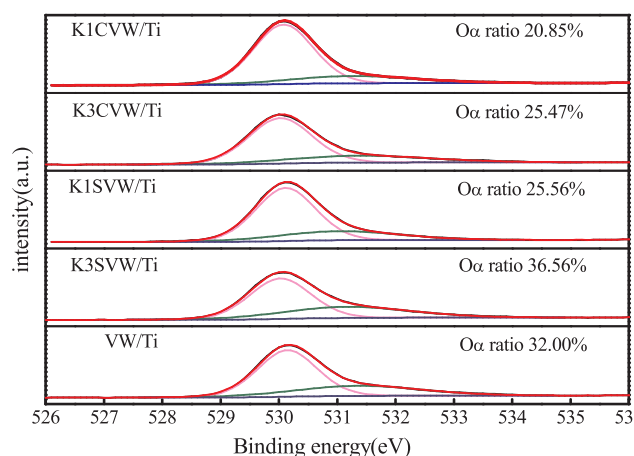


Fig. 9. XPS spectra of the  $\text{O}_{1s}$  peaks of V/W-Ti, K1,3SV/W-Ti, K1,3CV/W-Ti.

It was concluded that when the catalyst was poisoned by KCl, the formed HCl would combine with the surface lattice oxygen and promote the formation of  $\text{O}_\alpha$ , thereby mitigating the effect of poisoning on mercury oxidation.

When  $\text{K}_2\text{SO}_4$  was loaded on the catalyst surface, the  $\text{O}_\alpha$  ratio varied from 32% (V/W-Ti) to 25.56% (K1SV/W-Ti) and 36.56% (K3SV/W-Ti), which indicated that  $\text{SO}_4^{2-}$  would also promote the generation of  $\text{O}_\alpha$ . Therefore, it was concluded that when the catalyst was poisoned by  $\text{K}_2\text{SO}_4$ , the  $\text{SO}_4^{2-}$  on the surface would greatly promote the formation of  $\text{O}_\alpha$ , thereby mitigating the effect of poisoning on mercury oxidation efficiency.

### 3.3.5. Mercury oxidation mechanism

Previous research [23] had described the mercury oxidation mechanism by the  $\text{V}_2\text{O}_5/\text{WO}_3\text{-TiO}_2$  catalyst with  $\text{O}_2$  and HCl present in the flue gas: First,  $\text{Hg}^0$  and HCl in the flue gas would adsorb on the active sites on the catalyst surface and form  $\text{V}_2\text{O}_3(\text{OH})_2\text{Cl}_2$  and  $\text{Hg}\cdots\text{O}\text{-V}^{4+}$ , respectively; they would interact with each other on the catalyst surface to form stable  $\text{HgCl}_2$ , which was then released to the flue gas; and the formed  $\text{V}_2\text{O}_3(\text{OH})_2$  will be oxidized by  $\text{O}_2$  to  $\text{V}_2\text{O}_5$ .

Fig. 10 shows the mercury oxidation mechanism of KCl and  $\text{K}_2\text{SO}_4$  poisoned catalysts. When K was loaded on the surface of catalyst and occupied the active sites, the adsorption capacity of  $\text{Hg}^0$  and the surface oxidation capacity were reduced, resulting in the catalyst deactivation. As shown in Fig. 10(a), when KCl was loaded on the  $\text{V}_2\text{O}_5/\text{WO}_3\text{-TiO}_2$  catalyst, not only would K combine with the Brønsted acid sites on the surface, but also the formed HCl would react with the active site and form  $\text{V}_2\text{O}_3(\text{OH})_2\text{Cl}_2$ , thus mitigating the effect of poisoning on mercury oxidation. As shown in Fig. 10(b), when  $\text{K}_2\text{SO}_4$  was loaded on the  $\text{V}_2\text{O}_5/\text{WO}_3\text{-TiO}_2$  catalyst, the  $\text{SO}_4^{2-}$  would promote the adsorption of  $\text{Hg}^0$  on the surface and the formation of chemisorbed oxygen species, and even  $\text{HgSO}_4$  was formed on the surface.

## 4. Conclusions

The mercury oxidation performance of KCl and  $\text{K}_2\text{SO}_4$  poisoned  $\text{V}_2\text{O}_5/\text{WO}_3\text{-TiO}_2$  catalysts was investigated in this paper. Mercury oxidation mechanism was derived for KCl and  $\text{K}_2\text{SO}_4$  poisoned catalysts after a series tests of XRD, BET, Hg-TPD, XPS. The key findings are concluded below:

1. The NO conversion efficiency would decrease as KCl or  $\text{K}_2\text{SO}_4$  was loaded on the catalysts. Besides, the NO conversion efficiency of KxCV/W-Ti was significantly lower than that of KxSV/W-Ti, because  $\text{SO}_4^{2-}$  on the catalyst surface improved the redox performance of the catalyst.
2. When the catalysts were poisoned by KCl, the mercury oxidation efficiency would decrease. When low amount of  $\text{K}_2\text{SO}_4$  (3%) was loaded onto the catalysts, the oxidation efficiency of  $\text{Hg}^0$  could be improved. However, the oxidation efficiency of mercury would also reduce when  $> 3\%$   $\text{K}_2\text{SO}_4$  was loaded.
3. The physical pore structure of the KCl and  $\text{K}_2\text{SO}_4$  poisoned catalysts surface did not change significantly, suggesting that KCl and  $\text{K}_2\text{SO}_4$  would cause no physical deactivation of the catalysts.
4. When the catalysts were poisoned by KCl, the K would occupy the active sites and reduce the adsorption of  $\text{Hg}^0$  on the surface. However, the generated HCl would be adsorbed on the surface forming  $\text{V}_2\text{O}_3(\text{OH})_2\text{Cl}_2$  that was the intermediate products for the  $\text{Hg}^0$  oxidation. It would alleviate the effect of catalyst deactivation on the oxidation of  $\text{Hg}^0$ .
5. When  $\text{K}_2\text{SO}_4$  was loaded onto the catalyst surface, the  $\text{SO}_4^{2-}$  would form strong acid sites on the catalyst surface promoting the adsorption of  $\text{Hg}^0$  and the formation of surface  $\text{O}_\alpha$ , and hence the oxidation of  $\text{Hg}^0$ .

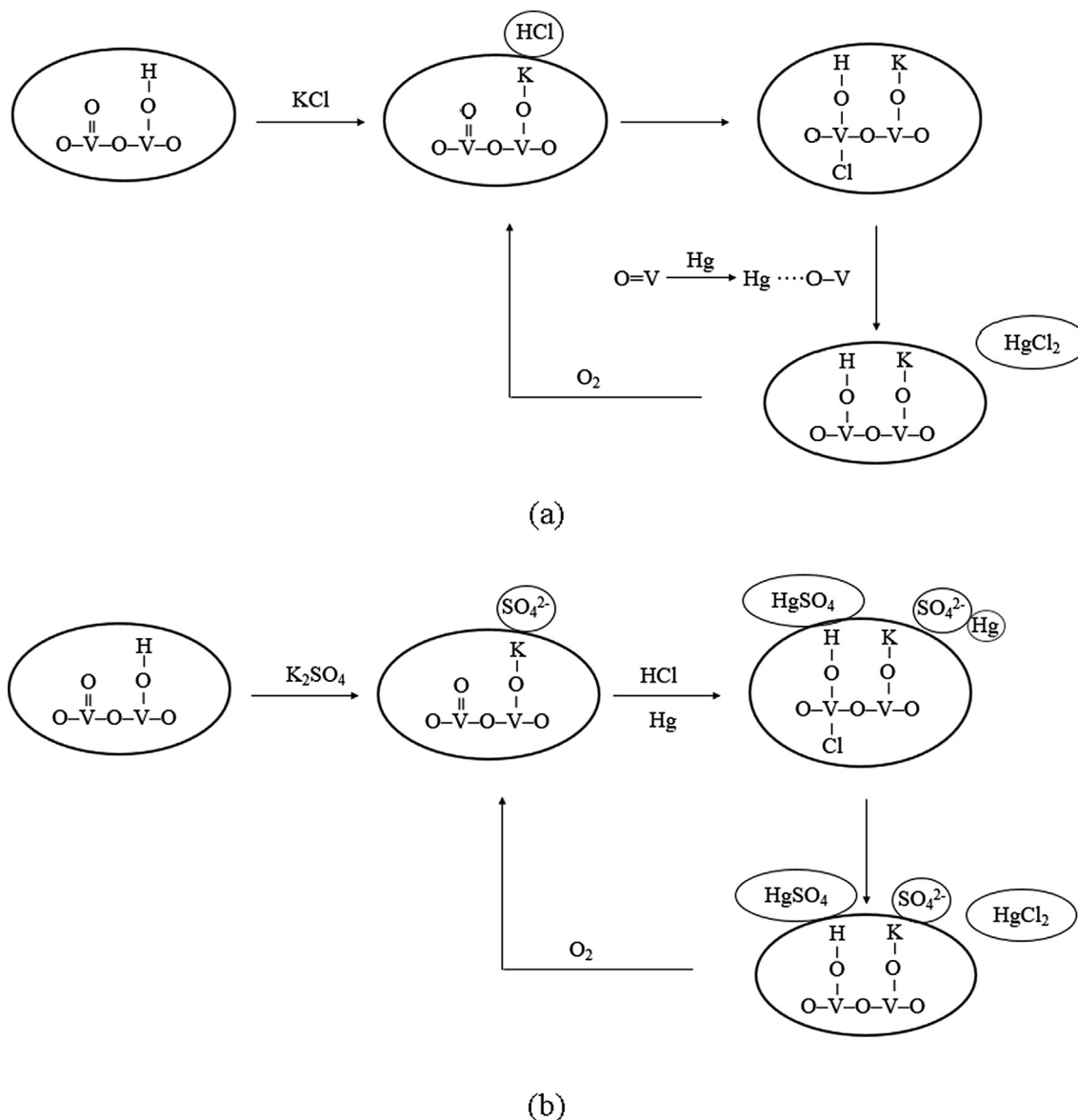


Fig. 10. Mercury oxidation mechanism:(a) KxCV/W-Ti; (b) KxSV/W-Ti.

#### CRediT authorship contribution statement

Jingyuan Hu, Guangqian Luo, Mengyuan Liu, Xian Li, Hong Yao conceived and designed the study. Jingyuan Hu performed the experiments. Jingyuan Hu, Zehua Li and Renjie Zou wrote the paper. Guangqian Luo, Xian Li, Hong Yao reviewed and edited the manuscript. All authors read and approved the manuscript.

#### Declaration of Competing Interest

The authors declare that they have no known competing financial interests or personal relationships that could have appeared to influence the work reported in this paper.

#### Acknowledgement

The National Key Research and Development Program of China (Grant No. 2016YFB0600603) and the National Natural Science Foundation of China (Grant No. 51776084) are gratefully acknowledged. The author also gratefully acknowledges the Analytical and Testing Center of Huazhong University of Science and technology of

experimental measurements.

#### References

- [1] Li Y, Zhang J, Zhao Y, et al. Volatility and speciation of mercury during pyrolysis and gasification of five Chinese coals. *Energy Fuels* 2011;25(9):3988–96.
- [2] UNEP. Global Mercury Assessment 2013: Sources, emissions, releases and environmental transport. Geneva, Switzerland: UNEP Chemicals Branch; 2013.
- [3] Zhao S, Duan Y, Yao T, et al. Study on the mercury emission and transformation in an ultra-low emission coal-fired power plant. *Fuel* 2017;199:653–61.
- [4] Senior CL, Sarofim AF, Zeng T, et al. Gas-phase transformations of mercury in coal-fired power plants. *Fuel Process Technol* 2000;63(2–3):197–213.
- [5] Zhou Q, Duan Y, Chen M, et al. Effect of flue gas component and ash composition on elemental mercury oxidation/adsorption by  $\text{NH}_4\text{Br}$  modified fly ash. *Chem Eng J* 2018;345:578–85.
- [6] Wang Z, Liu J, Zhang B, et al. Mechanism of heterogeneous mercury oxidation by HBr over  $\text{V}_2\text{O}_5/\text{TiO}_2$  catalyst. *Environ Sci Technol* 2016;50(10):5398–404.
- [7] Yang Z, Li H, Liu X, et al. Promotional effect of CuO loading on the catalytic activity and  $\text{SO}_2$  resistance of  $\text{MnO}_x/\text{TiO}_2$  catalyst for simultaneous NO reduction and  $\text{Hg}^0$  oxidation. *Fuel* 2018;227:79–88.
- [8] Yan N, Chen W, Chen J, et al. Significance of  $\text{RuO}_2$  modified SCR catalyst for elemental mercury oxidation in coal-fired flue gas[J]. *Environ Sci Technol* 2011;45(13):5725–30.
- [9] Zhou Z, Liu X, Hu Y, et al. Investigation on synergistic oxidation behavior of NO and  $\text{Hg}^0$  during the newly designed fast SCR process. *Fuel* 2018;225:134–9.
- [10] Casagrande L, Lietti L, Nova I, et al. SCR of NO by  $\text{NH}_3$  over  $\text{TiO}_2$ -supported

- V<sub>2</sub>O<sub>5</sub>-MoO<sub>3</sub> catalysts: reactivity and redox behavior. *Appl Catal B* 1999;22(1):63-77.
- [11] Aguilar-Romero M, Camposeco R, Castillo S, et al. Acidity, surface species, and catalytic activity study on V<sub>2</sub>O<sub>5</sub>-WO<sub>3</sub>/TiO<sub>2</sub> nanotube catalysts for selective NO reduction by NH<sub>3</sub>. *Fuel* 2017;198:123-33.
- [12] Du X, Gao X, Cui L, et al. Investigation of the effect of Cu addition on the SO<sub>2</sub>-resistance of a CeTi oxide catalyst for selective catalytic reduction of NO with NH<sub>3</sub>. *Fuel* 2012;92(1):49-55.
- [13] Munir S, Nimmo W, Gibbs BM. The effect of air staged, co-combustion of pulverised coal and biomass blends on NO<sub>x</sub> emissions and combustion efficiency. *Fuel* 2011;90(1):126-35.
- [14] Nussbaumer T. Combustion and co-combustion of biomass: fundamentals, technologies, and primary measures for emission reduction. *Energy Fuels* 2003;17(6):1510-21.
- [15] Kling Å, Andersson C, Myringer Å, et al. Alkali deactivation of high-dust SCR catalysts used for NO<sub>x</sub> reduction exposed to flue gas from 100 MW-scale biofuel and peat fired boilers: Influence of flue gas composition. *Appl Catal B* 2007;69(3-4):240-51.
- [16] Zheng Y, Jensen AD, Johnsson JE. Deactivation of V<sub>2</sub>O<sub>5</sub>-WO<sub>3</sub>-TiO<sub>2</sub> SCR catalyst at a biomass-fired combined heat and power plant. *Appl Catal B* 2005;60(3-4):253-64.
- [17] Larsson AC, Einvall J, Andersson A, et al. Physical and chemical characterisation of potassium deactivation of a SCR catalyst for biomass combustion. *Top Catal* 2007;45(1-4):149-52.
- [18] Zheng Y, Jensen AD, Johnsson JE. Laboratory investigation of selective catalytic reduction catalysts: Deactivation by potassium compounds and catalyst regeneration. *Ind Eng Chem Res* 2004;43(4):941-7.
- [19] Liu R, Xu W, Tong L, et al. Mechanism of Hg<sup>0</sup> oxidation in the presence of HCl over a commercial V<sub>2</sub>O<sub>5</sub>-WO<sub>3</sub>/TiO<sub>2</sub> SCR catalyst. *J Environ Sci* 2015;36:76-83.
- [20] Kong M, Liu Q, Zhu B, et al. Synergy of KCl and Hgel on selective catalytic reduction of NO with NH<sub>3</sub> over V<sub>2</sub>O<sub>5</sub>-WO<sub>3</sub>/TiO<sub>2</sub> catalysts. *Chem Eng J* 2015;264:815-23.
- [21] Zhao H, Bennici S, Shen J, et al. The influence of the preparation method on the structural, acidic and redox properties of V<sub>2</sub>O<sub>5</sub>-TiO<sub>2</sub>/SO<sub>4</sub><sup>2-</sup> catalysts. *Appl Catal A* 2009;356(2):121-8.
- [22] Zhang X, Huang Z, Liu Z. Effect of KCl on selective catalytic reduction of NO with NH<sub>3</sub> over a V<sub>2</sub>O<sub>5</sub>/AC catalyst. *Catal Commun* 2008;9(5):842-6.
- [23] Wan Q, Duan L, Li J, et al. Deactivation performance and mechanism of alkali (earth) metals on V<sub>2</sub>O<sub>5</sub>-WO<sub>3</sub>/TiO<sub>2</sub> catalyst for oxidation of gaseous elemental mercury in simulated coal-fired flue gas. *Catal Today* 2011;175(1):189-95.
- [24] Lee W, Bae GN. Removal of elemental mercury (Hg<sup>0</sup>) by nanosized V<sub>2</sub>O<sub>5</sub>/TiO<sub>2</sub> catalysts. *Environ Sci Technol* 2009;43(5):1522-7.
- [25] Granite EJ, Pennline HW, Hargis RA. Novel sorbents for mercury removal from flue gas. *Ind Eng Chem Res* 2000;39(4):1020-9.
- [26] Weckhuysen BM, Keller DE. Chemistry, spectroscopy and the role of supported vanadium oxides in heterogeneous catalysis. *Catal Today* 2003;78(1-4):25-46.
- [27] He S, Zhou J, Zhu Y, et al. Mercury oxidation over a vanadia-based selective catalytic reduction catalyst. *Energy Fuels* 2008;23(1):253-9.
- [28] Zhuang Y, Laumb J, Liggett R, et al. Impacts of acid gases on mercury oxidation across SCR catalyst. *Fuel Process Technol* 2007;88(10):929-34.
- [29] Eom Y, Jeon SH, Ngo TA, et al. Heterogeneous mercury reaction on a selective catalytic reduction (SCR) catalyst. *Catal Lett* 2008;121(3-4):219-25.
- [30] Quyang J, Hong D, Jiang L, et al. Effect of CO<sub>2</sub> and H<sub>2</sub>O on char properties. Part 1: pyrolysis char structure and reactivity. *Energy Fuels* 2020;34(4):4243-50. <https://doi.org/10.1021/acs.energyfuels.0c00032>.
- [31] Li Z, Zou R, Hong D, et al. Effect of CO<sub>2</sub> and H<sub>2</sub>O on char properties. Part 2: *in situ* and *ex situ* char in oxy-steam combustion. *Energy Fuels* 2020. <https://doi.org/10.1021/acs.energyfuels.0c00845>. In press.
- [32] Li Y, Murphy PD, Wu CY, et al. Development of silica/vanadia/titania catalysts for removal of elemental mercury from coal-combustion flue gas. *Environ Sci Technol* 2008;42(14):5304-9.
- [33] Pavlish JH, Sondreal EA, Mann MD, et al. Status review of mercury control options for coal-fired power plants. *Fuel Process Technol* 2003;82(2-3):89-165.
- [34] Wan Q, Duan L, He K, et al. Removal of gaseous elemental mercury over a CeO<sub>2</sub>-WO<sub>3</sub>/TiO<sub>2</sub> nanocomposite in simulated coal-fired flue gas. *Chem Eng J* 2011;170(2-3):512-7.
- [35] Lopez-Anton MA, Perry R, Abad-Valle P, et al. Speciation of mercury in fly ashes by temperature programmed decomposition. *Fuel Process Technol* 2011;92(3):707-11.
- [36] Wu Z, Jin R, Liu Y, et al. Ceria modified MnO<sub>x</sub>/TiO<sub>2</sub> as a superior catalyst for NO reduction with NH<sub>3</sub> at low-temperature. *Catal Commun* 2008;9(13):2217-20.
- [37] Li H, Wu S, Li L, et al. CuO-CeO<sub>2</sub>/TiO<sub>2</sub> catalyst for simultaneous NO reduction and Hg<sup>0</sup> oxidation at low temperatures. *Catal Sci Technol* 2015;5(12):5129-38.
- [38] Niksa S, Fujiwara N. A predictive mechanism for mercury oxidation on selective catalytic reduction catalysts under coal-derived flue gas. *J Air Waste Manag Assoc* 2005;55(12):1866-75.